

Integral relations and the adiabatic expansion method for 1+2 reactions above the breakup threshold: Helium trimers with soft-core potentials

E. Garrido

Instituto de Estructura de la Materia, CSIC, Serrano 123, E-28006 Madrid, Spain

C. Romero-Redondo

TRIUMF, 4004 Wesbrook Mall, Vancouver, BC, V6T 2A3, Canada

A. Kievsky and M. Viviani

Istituto Nazionale di Fisica Nucleare, Largo Pontecorvo 3, 56100 Pisa, Italy

The integral relations formalism introduced in [1, 2], and designed to describe $1+N$ reactions, is extended here to collision energies above the threshold for the target breakup. These two relations are completely general, and in this work they are used together with the adiabatic expansion method for the description of 1+2 reactions. The neutron-deuteron breakup, for which benchmark calculations are available, is taken as a test of the method. The s -wave collision between the ^4He atom and $^4\text{He}_2$ dimer above the breakup threshold and the possibility of using soft-core two-body potentials plus a short-range three-body force will be investigated. Comparisons to previous calculations for the three-body recombination and collision dissociation rates will be shown.

PACS numbers: 03.65.Nk, 21.45.-v, 31.15.xj, 34.50.-s

I. INTRODUCTION

Calculation of continuum states corresponding to processes where a particle hits a bound N -body system requires in principle knowledge of the corresponding $(1+N)$ -body wave function at large distances. Needless to say, the technical difficulties one has to face in order to obtain the wave function increase dramatically with N . In fact, already for $N=2$, calculation of the three-body wave function is far of being trivial.

However, even if knowledge of the $(1+N)$ -body wave function is unavoidable, the possibility of reducing the distance at which such wave function is needed is in itself an important step forward in the description of the reaction. As shown in [1, 2], this can indeed be done by means of two integral relations that are based on the Kohn Variational Principle. These two integral relations are a generalization to more than two particles of the integral relation given in [3, 4], and they permit to obtain the \mathcal{K} - (or \mathcal{S})-matrix of the reaction by using only the internal part of the wave function. Therefore, all the physical information concerning a given $1+N$ reaction can be obtained without an accurate knowledge of the asymptotic part of the wave function.

The fact that the asymptotic part is not needed anymore leads to a drastic reduction of the computer effort required to extract the \mathcal{K} -matrix. The only condition necessary to obtain accurate second-order estimates of the \mathcal{K} -matrix through the integral relations is that the trial wave function must fulfill the Schrödinger equation only in the interaction region. This means that, for instance, scattering states can be described with bound-state-like trial wave functions [5].

In [1, 2] the integral relations were implemented to describe $1+2$ reactions below the breakup threshold.

When used in combination with the hyperspherical adiabatic expansion method the dimension of the \mathcal{K} -matrix describing the reaction is dictated by the number of adiabatic potentials related to the possible outgoing elastic or inelastic channels, which typically is very small. Furthermore, thanks to integral relations, the convergence of the \mathcal{K} -matrix in terms of the adiabatic channels included in the expansion of the wave function is highly accelerated. Actually, the pattern of convergence is similar to the one found when the same method is used for the description of bound states [1, 2]. This is in fact not a minor issue, since as proved in [6], when used to describe low-energy scattering states, the convergence of the adiabatic expansion slows down significantly, even to the point that an accurate calculation of the \mathcal{K} -matrix would require infinitely many adiabatic terms in the expansion, what in practice makes the procedure useless.

The success of the method for energies below the breakup threshold immediately suggests its extension to describe low-energy breakup reactions. In this case the dimension of the \mathcal{K} -matrix is not finite, since contrary to the elastic and inelastic channels or transfer reactions, the full three-body continuum states are described by infinitely many adiabatic potentials.

The first goal of this work is to generalize the method described in [1, 2] for $1+N$ reactions to energies above the threshold for breakup of the bound target. This generalization will be shown in Section II, where a short summary of the method described in [2] will be given. In Section III, the $n-d$ reaction, for which a series of benchmark calculations are available [7, 8], will be used as a test of the method.

The second goal, which will be discussed in Section IV, concerns the use of the new method to investigate the $^4\text{He}+^4\text{He}_2$ atomic reaction above the dimer breakup

threshold. The case of the 0^+ state will be considered. In particular, we will focus on the use of soft-core ${}^4\text{He}$ - ${}^4\text{He}$ potentials. As shown in [9], the use of an attractive gaussian potential reproducing the same two-body properties as a standard hard-core potential (like for instance the LM2M2 potential) leads to equivalent bound three-body systems and phase-shifts for the elastic ${}^4\text{He}+{}^4\text{He}_2$ reaction, but only once that the soft-core potential is used together with a three-body short-term force. The possibility of using the same kind of potentials also to describe the breakup channel is interesting, since it automatically eliminates all the technical difficulties arising from the presence of a hard-core repulsion in the potential (see for instance Ref.[10]).

Finally, we close this work with a short summary and the conclusions.

II. FORMALISM

In Refs.[1, 2] $1+2$ reactions were described within the framework of the hyperspherical adiabatic expansion method for energies below the threshold for breakup of the dimer. Therefore, only elastic, inelastic, and transfer processes were possible. Since the formalism is described in great detail in Ref.[2], here we just summarize its main aspects, which are given in the first part of this section. In particular, we will focus on those key points that will permit an easier understanding of the generalization of the method to energies above the two-body breakup threshold, which will be shown in the second part of the section. In the last part we will describe the integral relations, which are actually the tools that permit to extract the \mathcal{K} -matrix of the reaction from the internal part of the wave functions.

A. Sketch of the method for energies below the breakup threshold

Given a three-body system, the corresponding wave function within the frame of the adiabatic expansion method is written as:

$$\Psi(\mathbf{x}, \mathbf{y}) = \frac{1}{\rho^5} \sum_{n=1}^{\infty} f_n(\rho) \Phi_n(\rho, \Omega), \quad (1)$$

where \mathbf{x} and \mathbf{y} are the usual Jacobi coordinates, and $\{\rho, \Omega\}$ are the hyperradius and the five hyperangles obtained from \mathbf{x} and \mathbf{y} [11]. The wave function has a well defined total angular momentum J , but for simplicity in the notation we omit this index (and its projection) in the expression above.

In hyperspherical coordinates the Hamiltonian operator $\hat{\mathcal{H}}$ takes the form:

$$\hat{\mathcal{H}} = -\frac{\hbar^2}{2m} \hat{T}_\rho + \hat{\mathcal{H}}_\Omega, \quad (2)$$

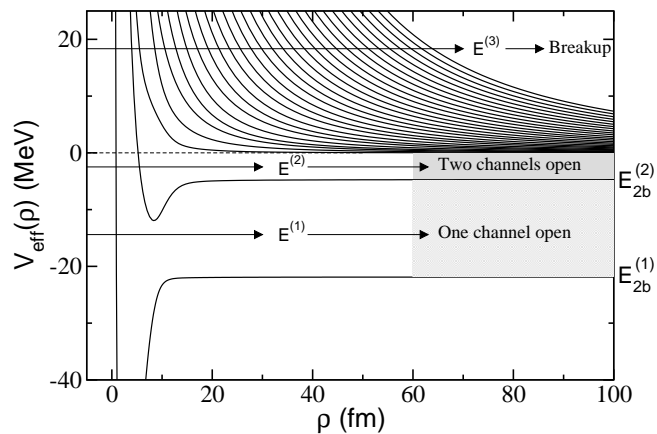


FIG. 1: Typical effective adiabatic potentials for a three-body system where two two-body bound states are present. The two lowest adiabatic potentials go asymptotically to the binding energies $E_{2b}^{(1)}$ and $E_{2b}^{(2)}$ of the two-body bound states. For a given three-body energy E , when $E_{2b}^{(1)} < E < E_{2b}^{(2)}$ only one channel is open, when $E_{2b}^{(2)} < E < 0$ both channels are open, and for $E > 0$ the breakup channel is also open.

where \hat{T}_ρ is the hyperradial kinetic energy operator, $\hat{\mathcal{H}}_\Omega$ contains all the dependence on the hyperangles, and m is an arbitrary normalization mass.

The angular functions $\Phi_n(\rho, \Omega)$, which form the complete basis used for the wave function expansion (1), are actually the eigenfunctions of $\hat{\mathcal{H}}_\Omega$,

$$\hat{\mathcal{H}}_\Omega \Phi_n(\rho, \Omega) = \frac{\hbar^2}{2m} \frac{1}{\rho^2} \lambda_n(\rho) \Phi_n(\rho, \Omega), \quad (3)$$

in such a way that the adiabatic effective potentials

$$V_{eff}^{(n)}(\rho) = \frac{\hbar^2}{2m} \left(\frac{\lambda_n(\rho) + \frac{15}{4}}{\rho^2} - Q_{nn}(\rho) \right) \quad (4)$$

enter in the coupled set of radial equations that permit to obtain the radial functions $f_n(\rho)$,

$$\begin{aligned} & \left[-\frac{d^2}{d\rho^2} + \frac{2m}{\hbar^2} (V_{eff}^{(n)}(\rho) - E) \right] f_n(\rho) \\ & + \sum_{n' \neq n} \left(-2P_{nn'} \frac{d}{d\rho} - Q_{nn'} \right) f_{n'}(\rho) = 0 \end{aligned} \quad (5)$$

where

$$Q_{nn'}(\rho) = \left\langle \Phi_n(\rho, \Omega) \left| \frac{\partial^2}{\partial \rho^2} \right| \Phi_{n'}(\rho, \Omega) \right\rangle_\Omega, \quad (6)$$

$$P_{nn'}(\rho) = \left\langle \Phi_n(\rho, \Omega) \left| \frac{\partial}{\partial \rho} \right| \Phi_{n'}(\rho, \Omega) \right\rangle_\Omega, \quad (7)$$

where the subscript Ω indicates integration over the hyperangles only (see [11] for details).

A typical behavior of the adiabatic potentials is shown in Fig.1. They correspond to a three-body system where two of the two-body subsystems have a bound state. This

is reflected in the fact that the two lowest effective adiabatic potentials go asymptotically to the binding energies $E_{2b}^{(1)}$ and $E_{2b}^{(2)}$ of each bound two-body system.

In the figure the different regions defined by the energy of the incident particles are depicted. All the three-body energies E such that $E_{2b}^{(1)} < E < E_{2b}^{(2)}$ (like $E^{(1)}$ in the figure) correspond to processes where only one channel is open. Only the elastic collision between the third particle and the bound two-body state with energy $E_{2b}^{(1)}$ is possible. When the three-body energy increases up to the region $E_{2b}^{(2)} < E < 0$ ($E^{(2)}$ in the figure) a second channel is open. Two different collisions are now possible, the one where a particle hits the bound state with binding energy $E_{2b}^{(1)}$, and the one where a particle hits the state with binding energy $E_{2b}^{(2)}$. In the same way, each of these reactions has two possible outgoing channels, corresponding to the two allowed bound two-body states and the third particle in the continuum. In other words, in this energy range the inelastic (if the two bound two-body states correspond to the same subsystem) or transfer (if the two bound two-body states correspond to different subsystems) channel is open. When $E > 0$ (like $E^{(3)}$ in the figure), the breakup channel is also open, and it is described by the remaining infinitely many adiabatic potentials.

The coupled system of radial equations (5) decouple asymptotically, and each of the radial wave functions behave at large distances as dictated by:

$$\left(-\frac{\hbar^2}{2m} \frac{d^2}{d\rho^2} + V_{eff}^{(n)}(\rho) - E \right) f_n(\rho) = 0. \quad (8)$$

When n corresponds to a closed channel the radial wave function f_n vanishes asymptotically. For values of E below the two-body breakup threshold, as considered in [2], and for a given incoming 1 + 2 channel, only outgoing 1 + 2 channels are allowed (either elastic, inelastic, or transfer). In this case, as shown in [11], the equation above describing the asymptotic behavior of the open-channel wave functions becomes

$$\left(\frac{d^2}{dy_n^2} + (k_y^{(n)})^2 - \frac{\ell_y(\ell_y + 1)}{y_n^2} \right) f_n(\rho) = 0, \quad (9)$$

where ℓ_y is the relative angular momentum between the dimer and the third particle, y_n refers to the modulus of the Jacobi coordinate between the center of mass of the outgoing bound two-body system and the third particle, and

$$k_y^{(n)} = \sqrt{\frac{2m}{\hbar^2} (E - E_{2b}^{(n)})}, \quad (10)$$

with $E_{2b}^{(n)}$ being the binding energy of the bound two-body system associated to the open channel n .

With this in hand, it is not difficult to see [2] that the asymptotic form of the corresponding three-body wave

function is given by:

$$\Psi_i \rightarrow \sum_{n=1}^{n_0} \left(A_{in}^{(K)} F_n^{(K)} + B_{in}^{(K)} G_n^{(K)} \right), \quad (11)$$

where i refers to the incoming channel, n_0 is the number of open channels (all of them 1 + 2 channels), and

$$F_n^{(K)} = \sqrt{k_y^{(n)}} j_{\ell_y}(k_y^{(n)} y_n) \frac{1}{\rho^{3/2}} \Phi_n(\rho, \Omega) \quad (12)$$

$$G_n^{(K)} = \sqrt{k_y^{(n)}} \eta_{\ell_y}(k_y^{(n)} y_n) \frac{1}{\rho^{3/2}} \Phi_n(\rho, \Omega), \quad (13)$$

where j_{ℓ} and η_{ℓ} are the usual regular and irregular Bessel functions (provided that we are dealing with short range potentials).

As shown in [2], Eq.(11) can be written in a compact matrix form as:

$$\Psi \rightarrow A^{(K)} F^{(K)} + B^{(K)} G^{(K)} = A^{(K)} \left(F^{(K)} - \mathcal{K} G^{(K)} \right), \quad (14)$$

where Ψ is a column vector with n_0 terms corresponding to the n_0 open channels, $A^{(K)}$ and $B^{(K)}$ are $n_0 \times n_0$ matrices made by the $A_{in}^{(K)}$ and $B_{in}^{(K)}$ elements in Eq.(11), and $F^{(K)}$ and $G^{(K)}$ are again column vectors whose n_0 terms are given by Eqs.(12) and (13).

From the equation above it is clear that the \mathcal{K} -matrix of the reaction is given by:

$$\mathcal{K} = -A^{(K)-1} B^{(K)}. \quad (15)$$

This matrix is real, and from it one can easily obtain the \mathcal{S} -matrix as $(1 + i\mathcal{K})(1 - i\mathcal{K})^{-1}$.

B. Generalization to energies above the breakup threshold

When the total three-body energy E in a 1+2 reaction is above the threshold for breakup of the dimer, the first consequence is that infinitely many adiabatic channels are then open (see Fig. 1 for $E = E^{(3)}$). Of course, still a finite number of them correspond to elastic, inelastic, or transfer processes, and the infinitely many remaining ones describe the breakup channel. Therefore, in this case the corresponding \mathcal{K} - (or \mathcal{S} -) matrix has infinite dimension.

In any case, for the finite open channels corresponding to outgoing 1 + 2 structures, the expressions given in the previous subsection are still valid. This means that for these particular outgoing channels the three-body wave function behaves asymptotically as given by Eq.(11), and Eqs.(12) and (13) are still valid.

On the other hand, the breakup channels are characterized by the fact that the effective potentials $V_{eff}^{(n)}$ associated to them go asymptotically to zero as:

$$V_{eff}^{(n)}(\rho) \xrightarrow{\rho \rightarrow \infty} \frac{\hbar^2}{2m} \frac{\left(K + \frac{3}{2}\right) \left(K + \frac{5}{2}\right)}{\rho^2}, \quad (16)$$

where K is the grand-angular quantum number defined as $2\nu + \ell_x + \ell_y$, where ℓ_x and ℓ_y are the orbital angular momenta associated to the Jacobi coordinates \mathbf{x} and \mathbf{y} , respectively, and $\nu = 0, 1, 2, \dots$. Therefore, asymptotically, each breakup adiabatic potential is associated to a fixed value of K . In fact, the corresponding angular eigenfunction $\Phi_n(\rho, \Omega)$ is, also asymptotically, a linear combination of hyperspherical harmonics with that particular value of K .

When inserting (16) into (8), we easily obtain that, asymptotically, the radial wave function for an outgoing breakup channel n satisfies the equation:

$$\left[\frac{d^2}{d\rho^2} + \kappa^2 - \frac{(K + \frac{3}{2})(K + \frac{5}{2})}{\rho^2} \right] f_n(\rho) = 0, \quad (17)$$

which is formally identical to the Eq.(9), which is satisfied by the radial wave functions associated to outgoing 1 + 2 channels, but replacing ℓ_y by $K + 3/2$, $k_y^{(n)}$ by $\kappa = \sqrt{2mE/\hbar^2}$, and y_n by ρ .

Therefore, in the more general case where the breakup channel is open, and assuming an incoming 1 + 2 channel i , the asymptotic form of the corresponding three-body wave function is given by:

$$\Psi_i \rightarrow \sum_{n=1}^{\infty} \left(A_{in}^{(K)} F_n^{(K)} + B_{in}^{(K)} G_n^{(K)} \right), \quad (18)$$

where $F_n^{(K)}$ and $G_n^{(K)}$ are still given by Eqs. (12) and (13), but of course, with the understanding that when n corresponds to an outgoing breakup channel the replacements $\ell_y \rightarrow K + 3/2$, $k_y^{(n)} \rightarrow \kappa$, and $y_n \rightarrow \rho$ have to be made (note that the relations $j_{K+\frac{3}{2}}(z) = \sqrt{\frac{\pi}{2z}} J_{K+2}(z)$ and $\eta_{K+\frac{3}{2}}(z) = \sqrt{\frac{\pi}{2z}} Y_{K+2}(z)$ permit to write Eqs.(12) and (13) in terms of the Bessel functions J_{K+2} and Y_{K+2} , which is how the asymptotic form of the breakup channels is usually presented in the literature).

Of course, the matrix form in Eq.(14) of the asymptotic wave function can still be used. As before, the \mathcal{K} -matrix of the reaction is given by $\mathcal{K} = -A^{(K)-1}B^{(K)}$, but now the matrices $A^{(K)}$ and $B^{(K)}$ have in principle infinite dimension and some truncation is then required.

Due to the fact that the hyperradius ρ appears as the natural radial coordinate describing the asymptotic behavior of the breakup channels, we then have that, for these channels, the adiabatic expansion is able to reach the correct asymptotic behavior for a sufficiently large, but finite, value of ρ . For this reason, for processes without 1 + 2 open channels ($3 \rightarrow 3$ processes), the \mathcal{K} -matrix could in principle be extracted with sufficient accuracy from the asymptotic behavior. However, this is not true when 1 + 2 channels are open. For these channels the correct asymptotic form (described by (12) and (13)) can not be reached until the Jacobi coordinate y and hyperradius ρ are equal, which only happens at infinity. Therefore it is essential in this case to use a formalism in which the \mathcal{K} -matrix is not extracted from the asymptotic part of the wave function but from its internal part.

C. Integral relations

The derivation of the integral relations has been shown in Ref.[2]. This derivation is completely general, and it is not particularized to the case of incident energies below the breakup threshold. Therefore, the same expressions derived in [2] apply when the breakup channel is open. According to it, by making use of the Kohn Variational Principle, it has been proved that when using a trial three-body wave function Ψ^t , one can obtain the matrices $A^{(K)}$ and $B^{(K)}$ accurate up to second order in $\delta(\Psi - \Psi^t)$, and their matrix elements are given by:

$$B_{ij} = \frac{2m}{\hbar^2} \langle \Psi_i^t | \hat{\mathcal{H}} - E | F_j^{(K)} \rangle \quad (19)$$

$$A_{ij} = -\frac{2m}{\hbar^2} \langle \Psi_i^t | \hat{\mathcal{H}} - E | G_j^{(K)} \rangle, \quad (20)$$

where Ψ_i^t describes each possible incoming channel and the index j refers to each possible outgoing channel (either 1 + 2 or breakup).

In this work, the trial three-body wave function will be the one obtained as sketched in subsection II A. To be precise, it will be obtained by solving the Faddeev equations by means of the hyperspherical adiabatic expansion method (see Ref.[11] for details).

Since the regular and irregular functions $F^{(K)}$ and $G^{(K)}$ are asymptotically solutions of $(\mathcal{H} - E)F^{(K)}, G^{(K)} = 0$, it is then clear that the integral relations (19) and (20) depend only on the short-range structure of the scattering wave function Ψ^t .

It is important to note that the function $G^{(K)}$, defined in Eq.(13), is irregular at the origin. In order to avoid the problems arising from this fact, the $G^{(K)}$ function is regularized. This means that in Eq.(20) the Bessel function η contained in $G^{(K)}$ is actually replaced by another function that goes to zero at the origin and behaves exactly as η at large distances. In [2] this was done by using $\tilde{\eta}_\ell(z) = (1 - e^{-\gamma z})^{\ell+1} \eta_\ell(z)$, where $\gamma (> 0)$ is a parameter. However, in our case, where the index ℓ can reach pretty high values ($\ell = K + 3/2$ in the breakup channels) this procedure is not appropriate.

In this work we have regularized the irregular Bessel function by solving Eq.(8) for each individual adiabatic potential. The solutions of this equation behave asymptotically as $f_n(z) \rightarrow z j_\nu(z) - \tan \delta_n z \eta_\nu(z)$, where δ_n is the phase-shift, and the index ν is equal to ℓ_y for the 1 + 2 channels, and $K + 3/2$ for the breakup channels. Then, the irregular Bessel function implicitly contained in Eq.(20) is replaced by:

$$\tilde{\eta}_\nu(z) = \frac{z j_\nu(z) - f_n(z)}{z \tan \delta_n}, \quad (21)$$

which by construction is regular at the origin and goes asymptotically to $\eta_\nu(z)$.

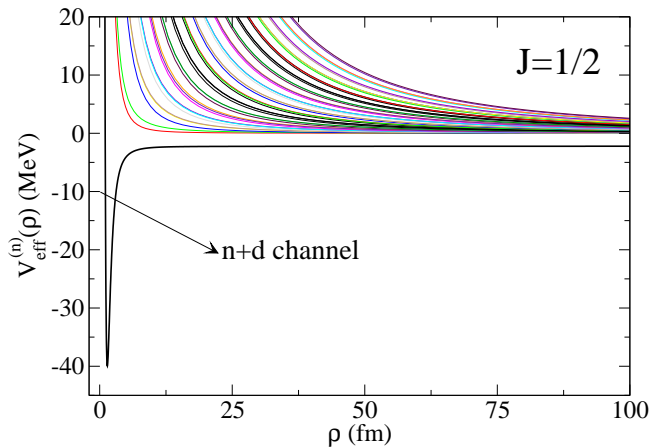


FIG. 2: (Color online) Effective adiabatic potentials for the neutron-neutron-proton system in the doublet case. The thick curve corresponds to the neutron+deuteron channel, and it goes asymptotically to the deuteron binding energy. All the remaining adiabatic potentials correspond to breakup channels.

III. A TEST CASE: NEUTRON-DEUTERON SCATTERING

The benchmark solutions for neutron-deuteron breakup amplitudes are shown in [7, 8]. For this reason we take this case as a test for the method shown in this work.

In particular, the nucleon-nucleon interaction is chosen to be the revised Malfliet-Tjon I-III model s -wave potential [7], which for the spin triplet and singlet cases takes the form:

$$V_t(r) = \frac{1}{r} (-626.885e^{-1.55r} + 1438.72e^{-3.11r}) \quad (22)$$

$$V_s(r) = \frac{1}{r} (-513.968e^{-1.55r} + 1438.72e^{-3.11r}), \quad (23)$$

where r is given in fm, and the potential in MeV. Also, $\hbar^2/m=41.47$ MeV fm². The potential above leads to a binding energy for the deuteron of 2.2307 MeV.

In the calculation only s -waves are considered. Therefore, two different total angular momenta are possible, the quartet case ($J = 3/2$), for which only the triplet s -wave potential (22) enters, and the doublet case ($J = 1/2$), for which both, the singlet and the triplet potentials contribute. In Fig.2 we show the computed adiabatic effective potentials (Eq.(8)) for the doublet case. As you can see, they follow the general trend of the potentials shown in Fig.1, although in this case there is only one $1+2$ channel, which corresponds to the neutron-deuteron reaction that we want to investigate. The corresponding adiabatic potential is given by the thick-solid line in the figure, and it will be labeled as channel 1. As expected, the asymptotic value of this potential corresponds to the binding energy of the deuteron.

TABLE I: Inelasticity parameter $|\mathcal{S}_{11}|$ for the neutron-deuteron scattering for two different laboratory neutron beam energies (14.1 MeV and 42.0 MeV) for the doublet and quartet cases. The value of K_{\max} is the K -value associated to the last adiabatic potential included in the calculation. The numbers within parenthesis have been obtained without use of the integral relations. The last row gives the value quoted in Ref.[8].

K_{\max}	Doublet		Quartet	
	14.1 MeV	42.0 MeV	14.1 MeV	42.0 MeV
4	0.4662 (0.4710)	0.4929 (0.4719)	0.9794 (0.9809)	0.8975 (0.8865)
8	0.4637 (0.4670)	0.4993 (0.4985)	0.9784 (0.9794)	0.9026 (0.9050)
12	0.4640 (0.4664)	0.5014 (0.5041)	0.9783 (0.9792)	0.9030 (0.9071)
16	0.4643 (0.4666)	0.5019 (0.5051)	0.9782 (0.9792)	0.9031 (0.9071)
20	0.4644 (0.4666)	0.5021 (0.5052)	0.9782 (0.9791)	0.9033 (0.9069)
24	0.4645 (0.4666)	0.5022 (0.5055)	0.9782 (0.9790)	0.9033 (0.9071)
28	0.4645 (0.4667)	0.5022 (0.5056)	0.9782 (0.9790)	0.9033 (0.9071)
Ref.[8]	0.4649	0.5022	0.9782	0.9033

A. Inelasticity and phase-shifts

The unitarity of the \mathcal{S} -matrix implies that given an incoming channel, for instance channel 1 ($n+d$ channel), we have that $\sum_1^\infty |\mathcal{S}_{1n}|^2 = 1$, or, in other words,

$$\sum_{n=2}^\infty |\mathcal{S}_{1n}|^2 = 1 - |\mathcal{S}_{11}|^2, \quad (24)$$

which means that an accurate calculation of the elastic term \mathcal{S}_{11} amounts to an accurate calculation of the infinite summation of the $|\mathcal{S}_{1n}|^2$ terms ($n > 1$) corresponding the breakup channels.

Also, the complex value of \mathcal{S}_{11} can be written in terms of a complex phase-shift δ as:

$$\mathcal{S}_{11} = e^{2i\delta} = e^{-2\text{Im}(\delta)} e^{2i\text{Re}(\delta)} = |\mathcal{S}_{11}| e^{2i\text{Re}(\delta)}. \quad (25)$$

The value of $|\mathcal{S}_{11}|^2$ gives the probability of elastic neutron-deuteron scattering, and $|\mathcal{S}_{11}|$ is what usually referred to as the inelasticity parameter (denoted by η in [7, 8]). Obviously, the closer the inelasticity to 1 the more elastic the reaction. In fact, for energies below the breakup threshold the phase-shift is real and $|\mathcal{S}_{11}| = 1$.

In Table I we give the inelasticity parameter $|\mathcal{S}_{11}|$ for the two laboratory neutron energies used in [8], i.e., 14.1 MeV and 42.0 MeV. We have computed the inelasticity parameter for both, the doublet and the quartet states. We give the computed values of $|\mathcal{S}_{11}|$ for different truncations in the infinite summation (18). In particular, in the

TABLE II: The same as Table I for $\text{Re}(\delta)$.

K_{max}	Doublet		Quartet	
	14.1 MeV	42.0 MeV	14.1 MeV	42.0 MeV
4	105.82 (97.62)	42.66 (28.89)	69.04 (60.88)	38.98 (25.29)
8	105.57 (99.91)	41.65 (32.88)	68.99 (63.24)	37.95 (28.98)
12	105.53 (101.01)	41.49 (34.80)	68.98 (64.43)	37.77 (31.07)
16	105.53 (101.68)	41.46 (36.05)	68.97 (65.11)	37.73 (32.28)
20	105.53 (102.12)	41.45 (36.81)	68.96 (65.54)	37.72 (33.03)
24	105.53 (102.41)	41.44 (37.30)	68.96 (65.84)	37.71 (33.55)
28	105.53 (102.49)	41.44 (37.90)	68.96 (65.88)	37.71 (33.58)
Ref.[8]	105.50	41.37	68.96	37.71

table we give the value K_{max} of the asymptotic grand-angular quantum number associated to the last adiabatic potential included in the calculation (see Eq.(16)). The values given in the table without parenthesis have been obtained by using the integral relations (19) and (20), while the ones within parenthesis have been calculated from the $A^{(K)}$ and $B^{(K)}$ matrices extracted directly from the asymptotic part of the three-body wave function, as indicated in Eq.(14). The last row in the table gives the value obtained in [8].

As seen in the table, when using the integral relations the agreement with the results in [8] is very good. Actually, we obtain precisely the same result for the two energies in the quartet case, and a tiny difference clearly smaller than 0.1% in the doublet case. Furthermore, the pattern of convergence is rather fast, specially in the quartet case, for which already for $K_{\text{max}} = 8$ we obtain a result that can be considered very accurate. In the doublet case the convergence is a bit slower, and a value of K_{max} of about 16 is needed. As we can see from the values within parenthesis, when the integral relations are not used, the value of $|\mathcal{S}_{11}|$ seems to converge more slowly, and even if converged, the result is less accurate.

From Eq.(25) we have that, together with the inelasticity parameter $|\mathcal{S}_{11}|$, a complete specification of the matrix element \mathcal{S}_{11} requires knowledge of the real part of the phase-shift $\text{Re}(\delta)$. The corresponding computed values are shown in Table II, where the meaning of the different columns is the same as in Table I. The behavior of $\text{Re}(\delta)$ is similar to what shown in Table I for $|\mathcal{S}_{11}|$. For the quartet case the same results as in [8] are obtained, while for the doublet again a very small difference smaller than 0.1% is again found. The pattern of convergence is also similar. A K_{max} value of 12 is already enough to get a quite accurate value. The main difference compared

to the results for $|\mathcal{S}_{11}|$ shown in Table I is that now the values of $\text{Re}(\delta)$ obtained without use of the integral relations are much less converged and much less accurate. The difference with the true result can reach up to 10%. This behavior was already observed in [1] for the phase-shift in a reaction below the breakup threshold. This is due to the fact that the hyperradius ρ and the Jacobi coordinate y entering in the asymptotic forms (12) and (13) are equivalent only at infinity as commented at the end of section II B. This means that a correct extraction of the phase-shift from the asymptotic part of the wave function requires to impose the boundary condition at infinity, for which also infinite adiabatic terms would be needed.

Therefore, for energies above the breakup threshold, the conclusion from Tables I and II is similar to the one reached in [1] for 1+2 elastic processes, that is, the use of the integral relations is crucial from two different points of view. First, it accelerates drastically the convergence of the values of the \mathcal{S} -matrix elements, and second, they are needed in order to obtain the correct result.

IV. SOFT-CORE ${}^4\text{He}$ - ${}^4\text{He}$ POTENTIAL AND THE ${}^4\text{He}$ - ${}^4\text{He}_2$ REACTION

Once the integral relations have been proved to be efficient in order to describe 1 + 2 reactions above the breakup threshold, in this section we shall use them to study the atomic ${}^4\text{He}$ - ${}^4\text{He}_2$ process. In particular, we shall focus on three-body states with spin and parity 0^+ , and the possibility of using simple two-body soft-core potentials will be investigated.

The ${}^4\text{He}$ - ${}^4\text{He}$ molecule is known to be one of the biggest diatomic molecules. Its binding energy has been estimated to be around 1 mK with a scattering length a around 190 a.u [12, 13]. Different accurate investigations of the ${}^4\text{He}$ - ${}^4\text{He}$ interaction are available in the literature [14–17]. All of them present the common feature of a sharp repulsion below an interparticle distance of approximately 5 a.u.. The presence of the repulsive core is the source of a series of important technical difficulties. For instance, the wave function in the inner regions, which is very small due to the large potential repulsion, is decisive for the energy of the bound states or the asymptotic properties of the continuum states. Therefore, the wave function must be calculated with high accuracy in this region, which typically requires a very important increase of the basis size. Furthermore, in case of using the adiabatic expansion method, the angular eigenvalues $\lambda_n(\rho)$ (see Eq.(3)) also diverge for small ρ , and this divergence provokes very frequent crossings between them that sometimes are not easy to handle [18].

In Ref.[9] the possibility of using a soft-core potential was investigated in the context of ${}^4\text{He}$ - ${}^4\text{He}_2$ collisions below the threshold for breakup of the dimer. In particular

the gaussian potential suggested in [18]

$$V_{2b}(r) = -1.227e^{-r^2/10.03^2} \quad (26)$$

was used (the strength of the potential is in K and the range in a.u.).

The dimer properties obtained with this potential are given in the second column in the upper part of table III. In particular, the dimer binding energy (E_{2b}), the two-body scattering length (a), the effective range (r_0), and the interatomic distance ($\langle r \rangle$) are given. The two parameters in the soft-core gaussian potential (26) were fitted to reproduce the scattering length and the effective range of the hard-core potential LM2M2 [14]. As seen in the third column of Table III (upper part), when this is done the binding energy E_{2b} and the interatomic distance $\langle r \rangle$ are also well reproduced.

However, even if both potentials have the same two-body properties, when moving to the three-body states important differences appear. The soft-core potential overbinds the two bound states in ${}^4\text{He}_3$ and the atom-dimer scattering length is clearly smaller (second and fourth columns in the lower part of Table III). In fact, as shown in [9], the phase-shifts obtained with these two potentials for the ${}^4\text{He}-{}^4\text{He}_2$ elastic scattering (below the breakup threshold) clearly differ from each other. As an example, for an incident energy of 1 mK, the phase-shifts obtained with the gaussian and the LM2M2 potentials are -56 and -63 degrees, respectively.

As also shown in [9], this anomalous behavior of the soft-core potential at the three-body level can be corrected by using a short-range effective three-body force, depending only on the hyperradius, that is added to the effective potential (4). In particular we choose the simple three-body force

$$W(\rho) = W_0 e^{-\rho^2/\rho_0^2}, \quad (27)$$

where the strength W_0 is adjusted to reproduce the trimer ground-state binding energy obtained with the LM2M2 potential. When this is done the results are fairly independent of the range parameter ρ_0 , at least within a reasonable value from $\rho_0 = 4$ a.u. to $\rho_0 = 10$ a.u.. The results given in the third column (lower part) of Table III have been obtained after inclusion of the three-body force. The precise values of W_0 and ρ_0 used are given in the first row of the lower part of the table. As we can see, once the binding energy of the ground state has been corrected, the binding energy of the excited state and the atom-dimer scattering length automatically agree with the corresponding values obtained with the LM2M2 potential. Furthermore, as seen in Fig.3 of [9], the low energy phase-shifts are also corrected when the effective three-body force is included.

The importance of the inclusion of the three-body force is also seen when investigating the ${}^4\text{He} - {}^4\text{He}_2$ reaction for incident energies ($E_i = E - E_{2b}$) above the threshold for breakup of the dimer, i.e., $E_i > |E_{2b}|$ (or $E > 0$). In Table IV we give the inelasticity ($|\mathcal{S}_{11}|$) and the real part

of the phase-shift ($\text{Re}(\delta)$) for energies $E = 5$ and $E = 25$ mK. As in Tables I and II, K_{max} is the grand-angular quantum number associated to the last adiabatic term included in the expansion (1). The boldface numbers have been obtained when the three-body force has been included in the calculation ($W_0 = 18.314$ K and $\rho_0 = 6$ a.u.), and the results within parenthesis have been obtained without the three-body force.

As we can see, the pattern of convergence is similar to the one observed in Tables I and II for the neutron-deuteron reaction. A K_{max} value of around 12 is enough to get a rather well converged inelasticity, while $\text{Re}(\delta)$ requires a few more adiabatic terms in order to reach convergence. Similarly to what found in [9] for energies below the breakup threshold, the inclusion of the three-body force gives rise to relevant changes in the computed values. These changes are particularly noticeable for $\text{Re}(\delta)$, which for the two energies under consideration increases up to 6 degrees when the three-body force is not included in the calculation. Also, we observe that for $E = 5$ mK the breakup probability ($1 - |\mathcal{S}_{11}|^2$) is still rather small, clearly smaller than 1% (with three-body force), while for $E = 25$ mK this probability rises up to 17% (12% without three-body force).

With the \mathcal{S} -matrix in hand, we can now compute the dissociation rate for the ${}^4\text{He} - {}^4\text{He}_2$ collision. The analytic form of this rate is given in Ref.[20], and for 0^+ states it becomes:

$$D_3 = \frac{\hbar\pi}{\mu_{1,23}k_{1,23}} (1 - |\mathcal{S}_{11}|^2), \quad (28)$$

where

$$\mu_{1,23} = \frac{2M_{\text{He}}}{3}, \quad k_{1,23}^2 = \frac{2\mu_{1,23}E_i}{\hbar^2}, \quad (29)$$

M_{He} is the mass of the ${}^4\text{He}$ atom, and $E_i = E - E_{2b}$ is the incident energy in the center of mass frame (E_{2b} is the binding energy of the ${}^4\text{He}_2$ dimer).

In Fig.3 we show the dissociation rate as a function of the three-body energy E . The thin-dashed and thin-solid lines are the results obtained with the gaussian soft-core potential (26) without and with the additional three-body force (27), respectively. The low energy behavior of the dissociation rate follows the E^{K_m+2} rule derived in [21], where K_m is the smallest grand-angular quantum number associated to the continuum adiabatic channels ($K_m = 0$ in our case of three indistinguishable bosons coupled to $J^\pi = 0^+$).

From the figure we can see that the effect of the three-body force is quite important. In fact, for small energies the three-body force reduces the rate by a factor of 2. At higher energies, beyond 10 mK, the effect is the opposite, and the three-body force increases the rate by a factor close to 1.5.

In Ref.[20] the same dissociation rate has been computed. The corresponding curve is shown in Fig.3 by the dotted curve. As we can see, there is an important difference compared to our calculation. Except at high

TABLE III: Helium dimer and helium trimer properties obtained with the soft-core potential in Eq.(26), the hard-core potential LM2M2 in Ref.[14], the modified soft-core potential (soft-core 2) in Eq.(30), and the hard-core SAPT potential in Ref.[17], respectively. The two-body properties are given in the upper part of the table, where E_{2b} , a , r_0 , and $\langle r \rangle$ are the dimer binding energy, the scattering length, the effective range, and the average interatomic distance, respectively. The three-body properties are given in the lower part, where $E_{3b}^{(g.s.)}$, $E_{3b}^{(exc.)}$, and a_0 are the binding energy of the trimer ground state, the binding energy of the trimer excited state, and the atom-dimer scattering length, respectively. For the soft-core and soft-core-2 potentials the column corresponding to the trimer properties has been split in two. The results given in the left part have been obtained without inclusion of any effective three-body force. The ones given in the right part are obtained after inclusion of a three-body force fitted to match the binding energy of the trimer ground state obtained with the LM2M2 [19] and SAPT [17, 20] potentials, respectively. The parameters used for the three-body potential are denoted by W_0 and ρ_0 (see Eq.(27)). All the distances are given in a.u. and the energies in mK, except W_0 which is given in K.

	Soft-core		LM2M2 [19]	Soft-core 2		SAPT [17, 20]
E_{2b} (mK)	-1.296		-1.302	-1.554		-1.564
a (a.u.)	189.95		189.05	174.09		173.50
r_0 (a.u.)	13.85		13.84	13.80		13.79
$\langle r \rangle$ (a.u.)	98.4		98.2	90.5		90.3
(W_0, ρ_0) (K, a.u.)	(0, -)	(18.314, 6)		(0, -)	(17.760, 6)	
$E_{3b}^{(g.s.)}$ (mK)	-150.0	-126.4	-126.4	-154.9	-130.9	-130.9
$E_{3b}^{(exc.)}$ (mK)	-2.467	-2.287	-2.265	-2.805	-2.612	-2.588
a_0 (a.u.)	165.9	210.6	224.3	181.7	226.0	226.8

TABLE IV: Inelasticity ($|\mathcal{S}_{11}|$) and real part of the phase-shift ($\text{Re}(\delta)$) for the ${}^4\text{He}-{}^4\text{He}_2$ collision at three-body energies (above threshold) $E = 5$ mK and $E = 25$ mK. The value of K_{max} is the K -value associated to the last adiabatic potential included in the calculation. The numbers within parenthesis have been obtained without inclusion of the three-body force.

K_{max}	$ \mathcal{S}_{11} $		$\text{Re}(\delta)$	
	$E = 5$ mK	$E = 25$ mK	$E = 5$ mK	$E = 25$ mK
4	0.9988 (0.9946)	0.9351 (0.9645)	69.30 (75.52)	35.09 (40.59)
8	0.9988 (0.9946)	0.9111 (0.9403)	69.23 (75.45)	34.80 (40.28)
12	0.9989 (0.9947)	0.9104 (0.9394)	69.20 (75.41)	34.63 (40.09)
16	0.9989 (0.9947)	0.9110 (0.9402)	69.17 (75.39)	34.60 (40.05)
20	0.9989 (0.9947)	0.9110 (0.9402)	69.16 (75.38)	34.59 (40.04)
24	0.9989 (0.9947)	0.9109 (0.9402)	69.15 (75.38)	34.58 (40.04)
28	0.9989 (0.9947)	0.9109 (0.9402)	69.15 (75.37)	34.58 (40.04)
40	0.9989 (0.9947)	0.9109 (0.9402)	69.15 (75.37)	34.58 (40.04)

energies ($E \gtrsim 10$ mK), where our result (with three-body force) and the one in [20] basically coincide, for small energies our rate is about a factor of 3 bigger.

However, we have to note that the hard-core two-body potential used in [20] gives rise to somewhat different

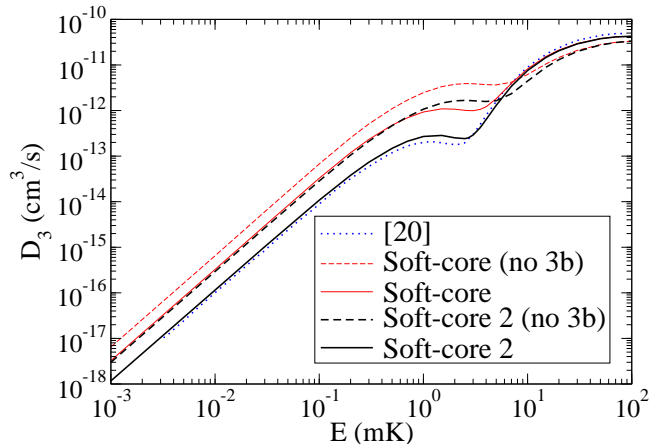


FIG. 3: (Color online) Dissociation rate (Eq.(28)) for the ${}^4\text{He} + {}^4\text{He}_2 \rightarrow {}^4\text{He} + {}^4\text{He} + {}^4\text{He}$ reaction as a function of the three-body energy E . The thin and thick curves have been obtained with the soft-core potential (26) and (30), respectively (see Table III). The dashed and solid curves are the results without and with inclusion of an effective three-body force. The dotted curve is the result given in [20].

dimer properties compared to the soft-core potential (26) and the LM2M2 potential [14]. In [20] they have used the potential based on the symmetry-adapted perturbation theory (SAPT) derived in [17]. The two-body properties obtained with this potential are given in the last column (upper part) of Table III. The two-body dimer is 20% more bound than with the LM2M2 potential, and therefore the scattering length and the interatomic distance are smaller than in the LM2M2 case.

To investigate the sensitivity of the dissociation rate

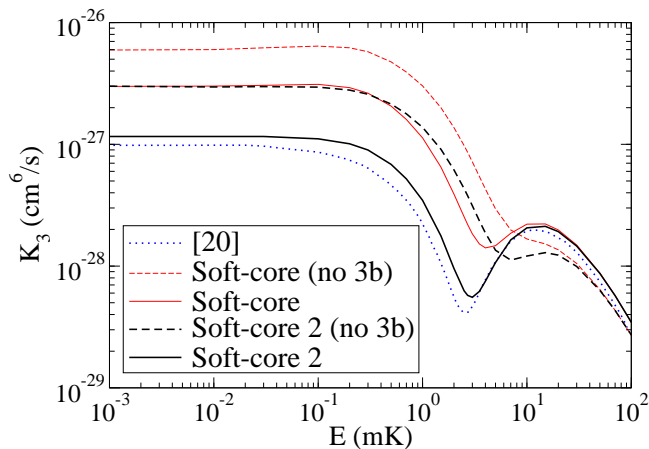


FIG. 4: (Color online) The same as Fig.3 for the recombination rate (Eq.(31)) for the process ${}^4\text{He} + {}^4\text{He} + {}^4\text{He} \rightarrow {}^4\text{He}_2 + {}^4\text{He}$.

to the details of the two-body interaction we have then constructed a second gaussian soft-core potential reproducing the two-body properties of the SAPT potential. This potential takes the form:

$$V_{2b}(r) = -1.234e^{-r^2/10.03^2}, \quad (30)$$

where the strength is given in K and the range in a.u.. The corresponding two-body properties are given in the fourth column (upper part) of Table III under the label “soft-core 2”. Again, when moving to the three-body system, this new soft-core potential presents the same deficiencies as the previous one, i.e., overbinding of the three-body bound states and a too small atom-dimer scattering length. As before, this problem is solved by inclusion of the three-body force, whose parameters are again fitted to reproduce the ground state binding energy of the helium trimer provided by the SAPT potential. The three-body properties with and without three-body force, as well as the parameters used for the three-body force are given in the last three columns (lower part) of Table III.

Making use of this new soft-core potential and the corresponding three-body force, we can compute again the dissociation rate (28). The results are shown in Fig.3 by the thick-dashed curve (no three-body force) and the thick-solid curve (with three-body force). The new rates are now smaller than the ones obtained with the previous soft-core potential. Furthermore, when the three-body force is included, and therefore not only the two-body properties but also the three-body ones agree with the ones obtained with the SAPT potential, our dissociation rate and the one given in [20] agree well for the whole range of energies. Only a small difference can be seen at about 1 mK. We can therefore see that the dissociation rate is very sensitive to the details of the two-body interaction. An additional 20% binding of the dimer, and the corresponding decrease in the scattering length, leads to a factor of 3 decrease in the rate.

The same conclusions are reached when investigating

the recombination rate corresponding to the inverse process ${}^4\text{He} + {}^4\text{He} + {}^4\text{He} \rightarrow {}^4\text{He}_2 + {}^4\text{He}$. This rate is given by the same \mathcal{S} -matrix elements as in the dissociation case, and its analytical form for three identical bosons with angular momentum and parity 0^+ is given by [20]:

$$K_3 = 3! \frac{32\hbar\pi^2}{\mu k^4} (1 - |\mathcal{S}_{11}|^2), \quad (31)$$

where

$$\mu^2 = \frac{M_{\text{He}}^2}{3}, \quad k^2 = \frac{2\mu E}{\hbar^2}, \quad (32)$$

M_{He} is the mass of the ${}^4\text{He}$ atom, and E is the total three-body energy.

The computed recombination rate is shown in Fig.4. The meaning of the curves is as in Fig.3. In Ref.[21] the recombination rate K_3 was proved to behave at low energies as E^{K_m} (K_m is the smallest grand-angular quantum number associated to the continuum adiabatic channels), which means that in our case, where $K_m = 0$, K_3 should be constant at very low energies, as observed in the figure. Again, inclusion of the three-body force reduces the rate by a factor of 2 to 3 at small energies (compare the dashed curves and the corresponding solid curves in the figure). Also, when the soft-core potential (30) together with the three-body force is used, the computed recombination rate agrees well with the rate given in [20] (dotted curve in the figure). This fact reveals again the importance of the fine details of the two-body interaction.

Finally, it is important to emphasize that in this work the \mathcal{S} -matrix has been obtained by use of the integral relations (19) and (20). As explained, they have the great advantage of needing only the internal part of the wave functions. In fact, the integrals involved in the calculations shown in this section can be safely performed with a maximum value for the hyperradius ρ of 4000 a.u.. Even less could be enough. However, in [20], where the adiabatic expansion was also used, the radial wave functions in Eq.(1) had to be expanded up to 5×10^5 a.u., which is definitely very delicate from the numerical point of view.

V. SUMMARY AND CONCLUSIONS

In this paper we have extended the use of the integral relations derived in [1, 2] to describe 1+2 reactions above the threshold for breakup of the dimer. As in [1, 2], the integral relations are used in combination with the adiabatic expansion method in order to construct the trial wave function. The main consequence of moving up to energies above the breakup threshold is that the \mathcal{S} -matrix describing the process has now infinite dimension. This was not the case for energies below the threshold, where the elastic, inelastic, or transfer channels were described by a finite (and small) number of adiabatic terms.

The applicability of the method has been tested with the neutron-deuteron reaction, for which benchmark cal-

culations are available. The agreement with these calculations is good, and the pattern of convergence is similar to the one found in [1, 2] for energies below the breakup threshold. The integral relations accelerate the convergence significantly, and typically about 10 adiabatic terms are enough to get a rather well converged result.

The method has then been used to investigate reactions involving three helium atoms. In particular we have focused on the possibility of using soft-core atom-atom potentials in order to describe the full process. These potentials permit to avoid all the technical problems arising from the use of more sophisticated potentials where a hard-core repulsion is always present. However, as already shown in [9], even if the soft-core potentials reproduce properly the dimer properties, an effective three-body force is needed in order to reproduce as well the properties of the trimer bound states and the atom-dimer scattering length obtained with the hard-core potentials.

We have found that the three-body force also modifies significantly the inelasticity and the phase-shift for energies above the breakup threshold. In fact, when computing the reaction rates for dissociation of the dimer (${}^4\text{He} + {}^4\text{He}_2 \rightarrow {}^4\text{He} + {}^4\text{He} + {}^4\text{He}$) and for the recombination process (${}^4\text{He} + {}^4\text{He} + {}^4\text{He} \rightarrow {}^4\text{He}_2 + {}^4\text{He}$) the three-body force decreases the rates even by a factor of 3 at low energies.

These two rates are also very sensitive to the details of the two-body interaction. We have found that a two-body potential, like the SAPT potential, providing a

dimer state about 20% more bound than the one obtained with the LM2M2 potential, also reduces the rates by a factor of around 3 at small energies. The soft-core potential reproducing the two-body properties of the SAPT potential, together with the corresponding three-body force designed to reproduce the trimer properties as well, gives then rise to reaction rates in very good agreement with the ones of the SAPT potential.

In summary, the integral relations are also useful in order to describe reactions above the breakup threshold. They accelerate significantly the convergence of the \mathcal{S} -matrix terms. For reactions involving hard-core two-body potentials, the use of soft-core potentials with the same two-body properties are a very good alternative, provided that they are used together with an effective three-body force designed to fit as well the bound state three-body energies. When this is done, the reaction rates obtained with the hard-core and the soft-core potentials agree pretty well. These rates are very sensitive to the details of the two-body interaction. Small variations of the dimer properties can produce sizable changes in the reaction rates at low energies.

Acknowledgments

This work was partly supported by funds provided by DGI of MINECO (Spain) under contract No. FIS2011-23565.

-
- [1] P. Barletta, C. Romero-Redondo, A. Kievsky, M. Viviani, E. Garrido, *Phys. Rev. Lett.* **103**, 090402 (2009).
- [2] C. Romero-Redondo, E. Garrido, P. Barletta, A. Kievsky, M. Viviani, *Phys. Rev. A* **83**, 022705 (2011).
- [3] F.E. Harris, *Phys. Rev. Lett.* **19**, 173 (1967).
- [4] A.R. Holt and B. Santos, *J. Phys. B* **5**, 497 (1972).
- [5] A. Kievsky, M. Viviani, P. Barletta, C. Romero-Redondo, E. Garrido, *Phys. Rev. C* **81**, 034002 (2010).
- [6] P. Barletta and A. Kievsky, *Few-Body Syst.* **45**, 25 (2009).
- [7] J.L. Friar *et al.*, *Phys. Rev. C* **42**, 1838 (1990).
- [8] J.L. Friar, G.L. Payne, W. Glöckle, D. Hüber, H. Witala, *Phys. Rev. C* **51**, 2356 (1995).
- [9] A. Kievsky, E. Garrido, C. Romero-Redondo, P. Barletta, *Few-body Syst.* **51**, 259 (2011).
- [10] F.M. Pen'kov, *J. Exp. Theor. Phys.* **97**, 485 (2003).
- [11] E. Nielsen, D.V. Fedorov, A.S. Jensen, and E. Garrido, *Phys. Rep.* **347**, 373 (2001).
- [12] F. Luo, C.F. Giese, and W.R. Gentry, *J. Chem. Phys.* **104**, 1151 (1996).
- [13] R.E. Grisenti, W. Schöllkopf, J.P. Toennies, G.C. Hegerfeldt, T. Köhler, and M. Stoll *Phys. Rev. Lett.* **85**, 2284 (2000).
- [14] Aziz R.A. and Slaman M.J., *J. Chem. Phys.* **94**, 8047 (1991).
- [15] K.T. Tang, J.P. Toennies, and C.L. Yiu, *Phys. Rev. Lett.* **74**, 1546 (1995).
- [16] T. Korona, H.L. Williams, R. Bukowski, B. Jeziorski, and K. Szalewicz, *J. Chem. Phys.* **106**, 5109 (1997).
- [17] M. Jeziorska, w. Cencek, K. Patkowsky, B. Jeziorski, K. Szalewicz, *J. Chem. Phys.* **127**, 124303 (2007).
- [18] E. Nielsen, D. V. Fedorov and A.S. Jensen, *J. Phys. B* **31**, 4085 (1998).
- [19] E.A. Kolganova, A.K. Motovilov, and W. Sandhas, *Phys. Part. and Nucl.* **40**, 206 (2009).
- [20] H. Suno and B.D. Esry, *Phys. Rev. A* **78**, 062701 (2008).
- [21] B.D. Esry, C.H. Greene, and H. Suno, *Phys. Rev. A* **65**, 010705 (2001).